Rayleigh-type Optical Mixing Signal Intensity Reconstruction From Sparse Data Using an Inverse Problem Approach

Cárdenas-García Jaime[1]; Paz José L.[1,2]; Costa Vera César[1,3]

[1]*Escuela Politécnica Nacional, Departamento de Física, Quito, Ecuador*
[2]*Departamento de Química, Universidad Simón Bolívar, Caracas, Venezuela*
[3]*GETNano, Universidad San Francisco de Quito, Ecuador*

Abstract: Previous work by one of the authors has shown the dependence of the Rayleigh-type optical mixing (RTOM) signal intensity on the incident pump and probe frequencies for different values of the ratio of relaxation times $k = T_1 / T_2$. In this work an inverse problem methodology is defined to determine the ratio of the relaxation times k from sparse and/or noisy incident pump and probe frequency data in order to reconstruct the full field RTOM signal intensity. The simulated results show a robust procedure which points to potential efficient experimental application, to be pursued in the near future.

Keywords: Rayleigh-type optical mixing, pump frequency, probe frequency, relaxation time, inverse problem.

Reconstrucción de la Intensidad de la Señal de Mezcla Tipo Rayleigh de Datos Escasos con Enfoque de Problema Inverso

Resumen: Trabajo previo de uno de los autores ha demostrado la dependencia de la intensidad de la señal de mezcla óptica tipo Rayleigh (RTOM) en la frecuencia de bombeo y de prueba para valores diferentes de relación de tiempos de relajación $k = T_1 / T_2$. En este trabajo se define una metodología de problema inverso para determinar la relación de tiempos de relajación k de datos incidentes, que son escasos y/o con ruido, de frecuencia de bombeo y de prueba que son usados para reconstruir la intensidad de la señal de RTOM de campo entero. Los resultados simulados demuestran un procedimiento robusto que apunta a una potencial aplicación experimental, que se la perseguirá en un futuro cercano.

Palabras clave: Mezcla óptica tipo Rayleigh, frecuencia de bombeo, frecuencia de prueba, tiempo de relajación, problema inverso.

1. INTRODUCTION

The study of nonlinear interaction of light with condensed matter is accomplished using different nonlinear spectroscopic techniques, including Rayleigh-type optical mixing (RTOM) spectroscopy which is useful for measuring ultrashort relaxation times in semiconductors and dye solutions (Yajima et al., 1978; Souma et al., 1980; Souma et al., 1982; Masumoto et al., 1985; Garcia Goulding and Marcano O., 1985; Paz et al., 1988). RTOM is a four-wave mixing technique that relies on a pump and a probe beam focused on the medium of interest resulting in a mixed frequency and wave vector signal (Yajima and Souma, 1978; Haroche and Hartman, 1972). The generation of the RTOM spectrum is accomplished by holding the frequency of one of the incident beams fixed for varying tuned (and not tuned) resonant frequency of the other incident beam. The resulting spectra allow an understanding of the nonlinear process used to generate the signal, and provide a method for measuring the population (T_1) and phase relaxation (T_2) times. A disadvantage in the experimental implementation of RTOM to obtain the complete spectrum is that the process is time intensive, if it is desired to have as comprehensive a spectrum as possible.

jfcardenasgarcia@gmail.com.

Previous work has shown the dependence of the RTOM signal intensity on the incident pump and probe frequencies for different values of the ratio of relaxation times $k = T_1 / T_2$ (Franco et al., 1990). This development makes it possible to theoretically generate the full signal intensity spectrum for a specified value of the ratio of relaxation times. From an experimental perspective it is useful to pose an inverse problem as to whether or not it might be possible using a sparse set of experimental spectral data to obtain an estimate of the ratio of the relaxation times, after which the full RTOM signal intensity spectrum is obtained, using the above referenced theoretical dependence.

2. THEORY

The theoretical background that leads to the formulation of the RTOM signal intensity is explicitly formulated in Franco et al. (1990), as a result only the relevant equations will be presented here. In particular, the normalized RTOM signal intensity, I_{norm}, is given by Equation (8) of Franco et al. (1990) and reproduced here, as seen Equation (1).

$$I_{norm} = \frac{I(\delta_1,\delta_2)}{I_{max}} \left\{ \frac{\left(\frac{1}{2k}\right)^2 [4+(\delta_1-\delta_2)^2]}{\left(\frac{1}{k}\right)^2 + (\delta_1-\delta_2)^2} \right\} \left\{ \frac{1/(1+\delta_2^2)}{(1+\delta_1^2)[1+(2\delta_1+\delta_2)^2]} \right\} \quad (1)$$

where the ratio of relaxation times is $k = T_1/T_2$, for frequency spaces $\Delta_1 = \omega_1 - \omega_0$ and $\Delta_2 = \omega_2 - \omega_0$, defined in terms of the pump frequency ω_1, probe frequency ω_2 and resonant frequency of the transition under study ω_0, yielding non-dimensional parameters $\delta_1 = \Delta_1 T_2$ and $\delta_2 = \Delta_2 T_2$. Figures 1(a)–1(c) shows 3D plots of the normalized intensity signal for $k = 0{,}1$; 1,0 and 10.0, respectively. Figures 2(a)–2(c) show the corresponding quantitative contour plots.

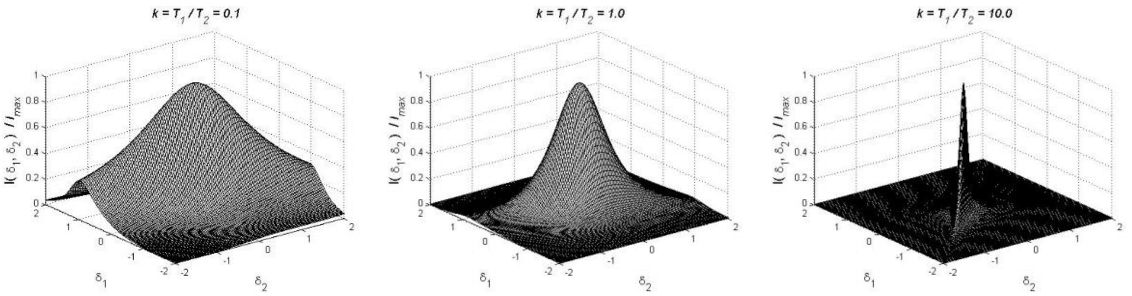

(a) (b) (c)

Figure 1(a) – 1(c). 3D plot of the RTOM signal intensity as a function of non-dimensional parameters $\delta_1 = \Delta_1 T_2$ and $\delta_2 = \Delta_2 T_2$ for the case of $k = 0{,}1; 1{,}0\ and\ 10{,}0$

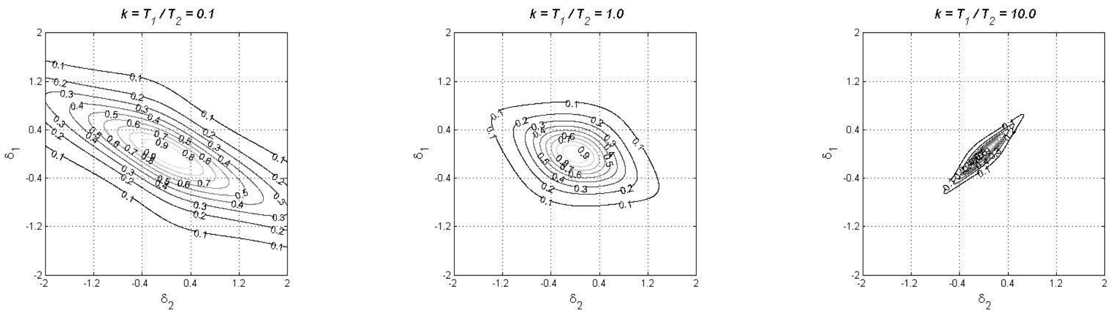

(a) (b) (c)

Figure 2(a) – 2(c). Contour plot of the RTOM signal intensity for $k = 0{,}1;\ 1{,}0$ and $10{,}0$

3. NON LINEAR LEAST SQUARES INVERSE PROBLEM METHODOLOGY

Traditionally theory and experimentation are done independently because of the rigor that each one requires. This dichotomy has led to an apocryphal Law of Research: Nobody believes the analytical/numerical results, except the person who generated them. Everybody believes the experimental results, except the person who obtained them. More recently, there is a greater tendency toward analytical/numerical simulations that rely on computation to generate large amounts of numerical data that need graphical representation for ease of analysis. Oftentimes the data generated is a full-field representation of the physical phenomena under consideration. This is equally true of experimental data such as interferometric or spectroscopic data that offers considerable amounts of data and even full-field images. Thus a need exists to develop approaches that take advantage of the strengths of analytical/numerical simulations and experimental results with the goal of combining them in a seamless manner to achieve what each of them alone is unable to achieve. One approach to satisfy this need is to develop an Inverse Problem Methodology (IPM) that takes into account that a dialectical dichotomy exists between forward or direct problems and reverse or inverse problems. Figure 3 shows how the direct and inverse problems may be defined for RTOM spectroscopy. The forward problem requires defining as inputs the experimental geometry, boundary conditions and the ratio of relaxation times $k = T_1 / T_2$ of the medium under consideration with resulting normalized RTOM signal intensity as output. The inverse problem starts out with normalized RTOM signal intensity for known experimental geometry and boundary conditions with the objective of recovering the ratio of relaxation times $k = T_1 / T_2$. Figures 1 – 2 show the results from solving the direct problem to obtain normalized RTOM signal intensity which shows a full-field representation for the limits of normalized non-dimensional parameters $\delta_1 = \Delta_1 T_2$ and $\delta_2 = \Delta_2 T_2$. The amount of data generated to make these plots can be varied greatly depending on the needs of the solution. The inverse problem starts out with full knowledge of the normalized RTOM signal intensity and asks the question as to whether or not it might be possible to make an accurate estimate of the ratio of relaxation times k, and more particularly what is the minimum sample size of data points required, where is the best area within the region delimited by normalized non-dimensional parameters δ_1 and δ_2 from which to sample, and even how noisy data affects the results.

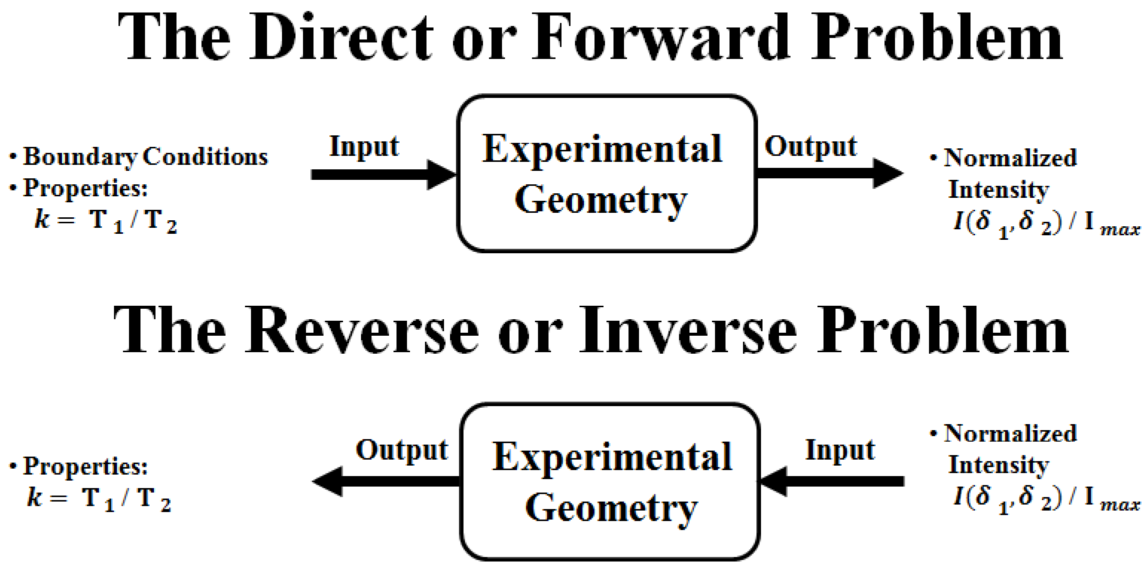

Figure 3. The Direct/Forward Problem and the Reverse/Inverse Problem

Figure 4 shows the virtual world of simulation and experimentation sides of the Forward Problem, which share similar characteristics. In both instances the problem needs to be defined including boundary conditions, geometry and medium properties; the analytical/numerical/experimental model needs to be developed with specific output parameters in mind; and finally, the input parameters are defined for which the solution and output parameters that are sought is implemented. What follows then is a process of verification and ascertaining that the model is working as it was designed to work, by examining the results and data generated, which are in the form of tables of data that are graphed or further numerically scrutinized with similar techniques, whether the results are from the simulation or the experimental side. Generally the simulation side is much more data robust than the experimental side, and typically a plot that combines the simulation and experimental results is generated to get a sense of the fit between theory and experiment, or the experimental results might be fit by a least squares approach to develop an empirical equation that is practical for applications. A question that might be asked at this point is whether or not it might be possible to use the experimental results to reproduce the relevant parameters of the model, in effect seeking to pose an Inverse Problem.

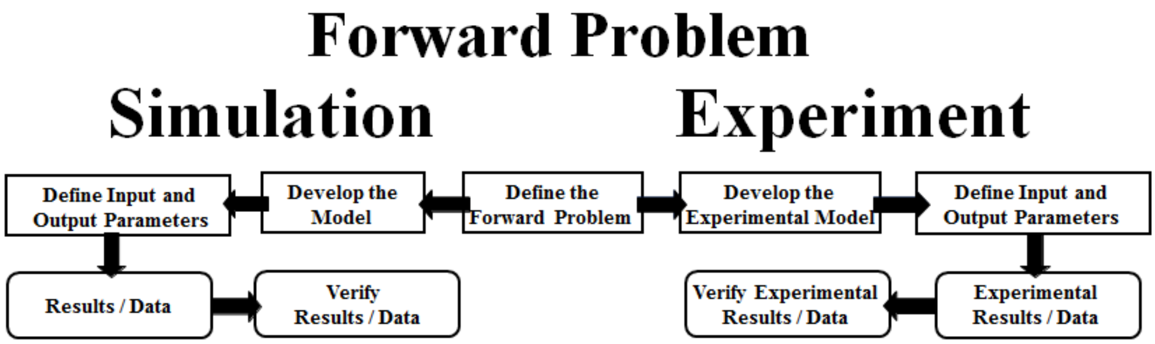

Figure 4. The Forward Problem as Simulation and Experiment

The simulation and experimentation sides of the Inverse Problem are shown in Figure 5. Central to the Inverse Problem implementation is a numerical non-linear least-squares Recursive Inverse Analysis, detailed below, that allows an over-determined set of results/data to be used and is capable of estimating several parameters of interest. Central to defining this Recursive Inverse Analysis is that an analytical/numerical model of the problem exists. Like the Forward Problem similar requirements have to be met on the simulation and the experimental sides: the Inverse Problem needs definition, calculation initiation parameters are set, results/data serve as inputs, and convergence criteria are specified. Also, it is possible to work on either the simulation side or the experimental side as needed, so as to complement the research needs. The simulation and experimentation sides of the Inverse Problem Methodology, which includes the Forward and Inverse Problems together, are shown in Figure 6. The purpose in representing them in this way is to show that it is possible to work only on the left or simulation side of this diagram, or only on the right side of the diagram, which relies on being able to model the phenomena of interest either analytically or numerically. This diagram brings into focus the fact that if a researcher is considering doing experimental work in order to resolve an inverse problem it might be useful to consider working on the left side of the equation to determine whether or not experimentation would be fruitful. Once it is shown that an inverse problem solution is possible on the simulation side of the diagram, including consideration of systematic and random errors, the requisite investment of equipment, supplies, time and effort can be more efficiently expended with a greater degree of certainty.

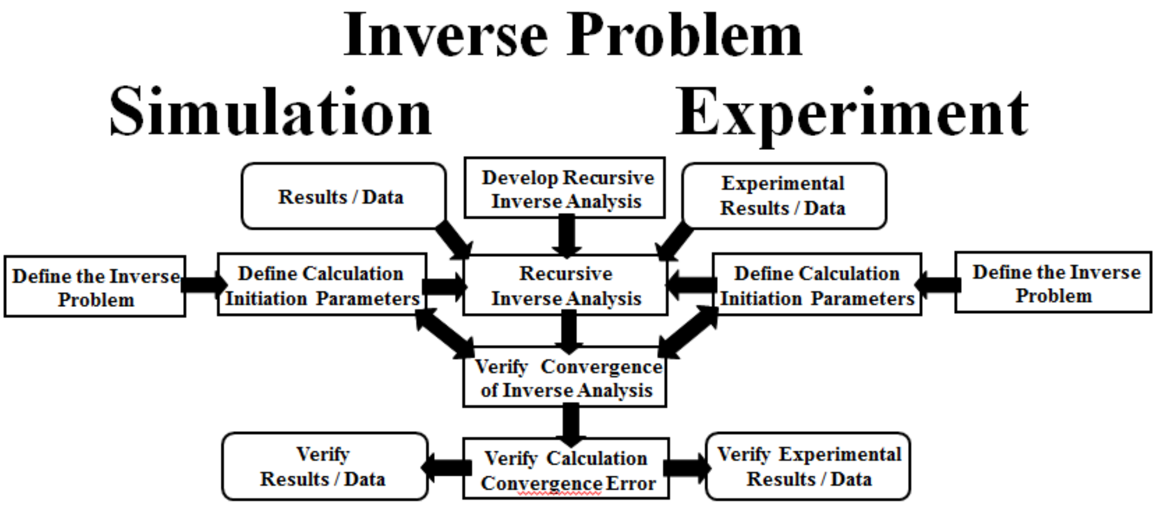

Figure 5. The Inverse Problem as Simulation and Experiment

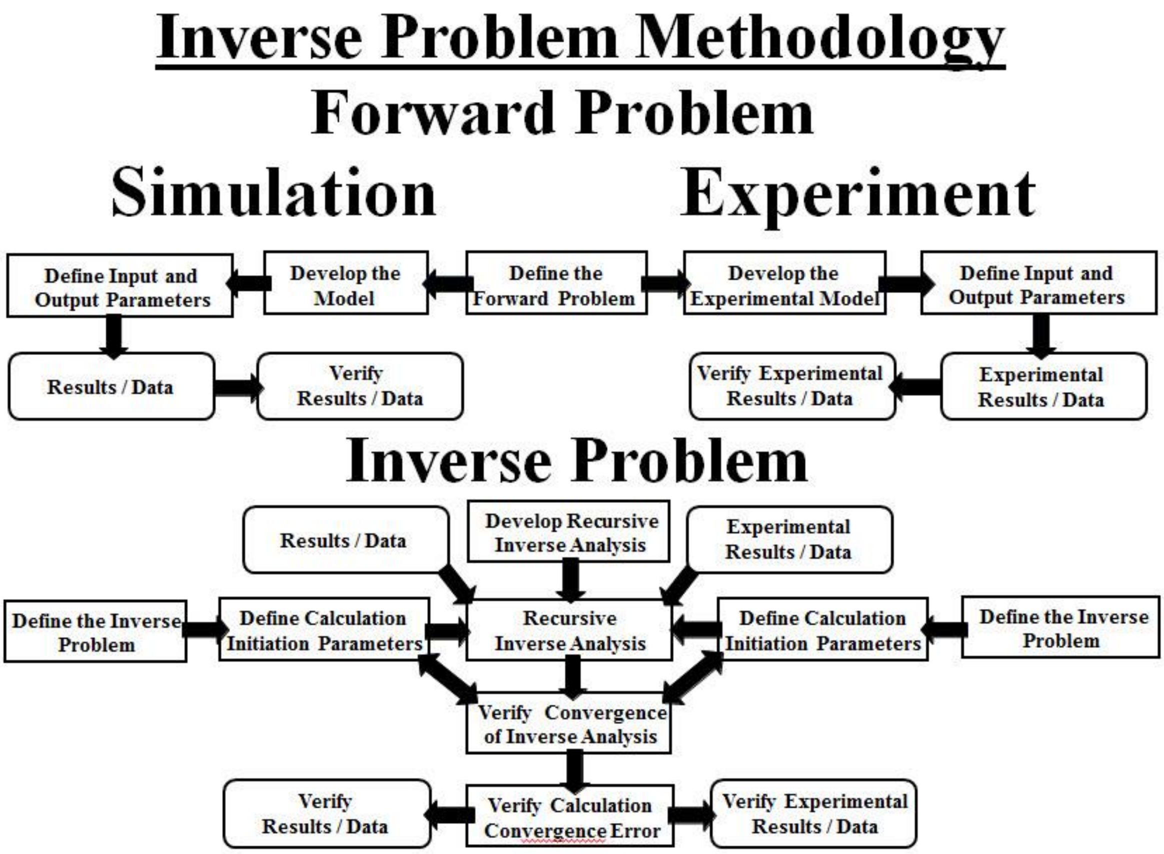

Figure 6. The Inverse Problem Methodology as Simulation and Experiment

3.1 Non-Linear Least-Squares Recursive Inverse Analysis

One approach to least-squares estimation of non-linear parameters relies on the expansion of the physical model as a Taylor series and calculating corrections to the several parameters at each iteration, assuming local linearity. The problem may be stated as follows [adapted from Marquardt (1963)]:

Let the physical model to fit the data be

$$E(y) = f(x_1, x_2, \cdots, x_m; \beta_1, \beta_2, \cdots, \beta_k) = f(\vec{x}, \vec{\beta}) \qquad (2)$$

where $x_1, x_2, \cdots, x_m$ are independent variables and $\beta_1, \beta_2, \cdots, \beta_k$ are the population values of k parameters, and $E(y)$ is the expected value of dependent variable y. Denoting data points by Equation (3),

$$\left(Y_i,\ X_{1i,} X_{2i,} \cdots, X_{ni}\right), \qquad \mathrm{i} = 1, 2, \cdots, \mathrm{n}. \qquad (3)$$

The objective is to compute the estimates of the parameters that minimize, as seen Equation (4)

$$\Phi = \sum_{i=1}^{n} \left[Y_i - \hat{Y}_i\right]^2 = \left\|\vec{Y} - \hat{\vec{Y}}\right\|^2 \qquad (4)$$

where $\hat{Y}_i$ is the value of y predicted by Equation (2) at the i^{th} data point.

One method based on expanding f in a Taylor's series expansion is the Gauss-Newton method (Hartley, 1961). Starting with a Taylor's series expansion of f which may be expressed as follows,

$$\langle Y(\vec{X}_i, \vec{b} + \vec{\delta}_t)\rangle = f(\vec{X}_i, \vec{b}) + \sum_{j=1}^{k} \left(\frac{\partial f_i}{\partial b_j}\right)_k (\delta_t)_j \qquad (5)$$

or,

$$\langle \vec{Y} \rangle = \vec{f}_0 + \vec{P}\,\vec{\delta}_t \qquad (6)$$

where $\vec{\beta}$ is replaced by $\vec{b}$, and the converged value of $\vec{b}$ is the least-squares estimate of $\vec{\beta}$. The small vector $\vec{\delta}_t$ is a small correction to $\vec{b}$. The brackets ‹› distinguish predictions based on the linearized model from those based upon the actual nonlinear model. As a result the value of Φ predicted by Equation (5) is Equation (7),

$$\Phi = \sum_{i=1}^{n} [Y_i - \langle Y_i \rangle]^2. \qquad (7)$$

Since $\vec{\delta}_t$ appears linearly in Equation (6) it can be found by setting $\partial\langle\Phi\rangle/\partial\delta_j = 0$, for all j, and $\vec{\delta}_t$ is found solving

$$A\vec{\delta}_t = \vec{g}_t \qquad (8)$$

Where, Equations from (9) to (11b)

$$A^{(kxk)} = P^T P \qquad (9)$$

$$P^{(nxk)} = \left(\frac{\partial f_i}{\partial b_j}\right), \quad \mathrm{i} = 1, 2, \cdots, \mathrm{n};\ \mathrm{j} = 1, 2, \cdots, \mathrm{k}, \qquad (10)$$

$$\vec{g}^{(kx1)} = \left(\sum_{i=1}^{n} (Y_i - f_i)\left(\frac{\partial f_i}{\partial b_j}\right)\right), \quad \mathrm{j} = 1, 2, \cdots, \mathrm{k}, \qquad (11a)$$

$$= P^T\left(\vec{Y} - \vec{f}_0\right) \qquad (11b)$$

The above least-squares estimation of non-linear parameters is presented to formalize the process of how this is accomplished. A practical way to accomplish this least-squares estimation of non-linear parameters procedure more efficiently and robustly is to use a MATLAB® script that is able to solve these problems with time-tested and standardized procedures.

3.2 Estimation of the Ratio of Relaxation Times from Normalized RTOM Signal Intensity

The particular inverse problem that is solved is to find an estimate the ratio of relaxation times $k = T_1/T_2$ from values of the normalized RTOM signal intensity defined by the normalized non-dimensional parameters δ_1 and δ_2. From an experimental perspective, the usual practice is to fix the pump frequency ω_1 and to change the probe frequency ω_2, or vice versa, as the medium is interrogated by measuring the intensity of the RTOM spectrum which is then normalized with respect to the maximum intensity. One way to lend efficiency to this procedure is to make the number of RTOM spectrum intensity measurements is as sparse as possible, but sufficient to allow for the robust estimation of the ratio of relaxation times $k = T_1/T_2$. Additionally, it would make sense to determine which values of pump frequency ω_1 and probe frequency ω_2 yield the best estimates of k, and even how noisy data affects the results, all this on the simulation side, for guidance leading to experimentally obtained results.

3.3 Simulation Results

Table 1 shows the results of estimating k by using data sets of varying sizes from 5 to 201 data points, as well as tabulating the number of iterations needed for obtaining the k. The data points are evenly distributed along δ_2 at fixed δ_1. Since all of the estimates for k are exact to four decimals, the parameter used to determine the near optimum number of data points for all values of k is the number of iterations, which is a minimum for data set 7 (in yellow) which corresponds to 41 data points.

A similar result is shown in Table 2 for data points evenly distributed along δ_1 at fixed δ_2, where again data set 7 (in yellow) is shown to require the minimum number of iterations.

Table 1. Parameter estimate of $k = T_1/T_2$ for fixed $\delta_1 = 0{,}50$

	k	**0,10**		**1,00**		**10,00**	
Data Set	**Number of Data Points**	**Number of Iterations**	**Parameter Estimate**	**Number of Iterations**	**Parameter Estimate**	**Number of Iterations**	**Parameter Estimate**
1	5	27	0,1000	34	1,0000	30	10,0000
2	9	33	0,1000	29	1,0000	33	9,9999
3	15	26	0,1000	31	1,0000	36	10,0000
4	19	27	0,1000	31	1,0000	40	10,0000
5	25	31	0,1000	36	1,0000	36	10,0000
6	31	29	0,1000	33	1,0000	36	10,0000
7	41	25	0,1000	31	1,0000	32	10,0000
8	51	24	0,1000	31	1,0000	34	10,0000
9	101	27	0,1000	27	1,0000	32	10,0000
10	201	23	0,1000	28	1,0000	33	10,0000

Table 2. Parameter estimate of $k = T_1/T_2$ for fixed $\delta_2 = 0{,}79$

	k	**0,10**		**1,00**		**10,00**	
Data Set	**Number of Data Points**	**Number of Iterations**	**Parameter Estimate**	**Number of Iterations**	**Parameter Estimate**	**Number of Iterations**	**Parameter Estimate**
1	5	26	0,1000	30	1,0000	38	10,0001
2	9	28	0,1000	27	1,0000	40	10,0002
3	15	32	0,1000	24	1,0000	36	10,0000
4	19	25	0,1000	29	1,0000	40	9,9999
5	25	32	0,1000	27	1,0000	36	10,0001
6	31	29	0,1000	26	1,0000	38	10,0000
7	41	23	0,1000	34	1,0000	35	10,0000
8	51	29	0,1000	29	1,0000	37	9,9999
9	101	25	0,1000	30	1,0000	37	10,0000

Figure 7(a)–(c) shows a qualitative result of adding noise to the normalized intensity and represented as contour maps for $k = 0{,}1$ and changing values of standard deviation, σ_{noise}, which as a measure of added random noise to the normalized intensity as per the Equation (12),

$$I_{norm} = I_{norm} + \sigma_{noise}\,(randn) \qquad (12)$$

where $randn$ is a MATLAB® random function that generates arrays of random numbers whose elements are normally distributed with mean 0, variance $\sigma^2 = 1$, and standard deviation $\sigma = 1$. The purpose of adding noise to the maximum normalized intensity is to assess the robustness of recovering an estimate of the ratio of relaxation times $k = T_1/T_2$, for changing values of σ_{noise}, the noise standard deviation.

Table 3 shows the results of estimating the ratio of relaxation times is k for increasing values of σ_{noise}, the noise standard deviation. This calculation is done using 41 data points evenly distributed along δ_2 at fixed δ_1. Recall that the use of 41 data points allowed a minimum number of iterations for convergence to obtain and estimate of k. Note from Table 3 that as the value of standard deviation increases, indicating an increasing level of noise, the number of iterations needed to obtain an estimate of k increases and the estimate of k diverges, sometimes significantly from the actual value.

An additional calculation done to determine whether or not there is a best region from which to acquire data in the range of values of δ_1 and δ_2 between -2 and +2 is shown in Figures 8–10. Regions of interest are defined by dividing the respective axes into twenty sections. This results in subdividing the total area under consideration into 400 sub-regions of interest. Within each sub-region the values of δ_1 and δ_2 were selected at random, so as to use them to generate 100 data points of normalized maximum intensity.

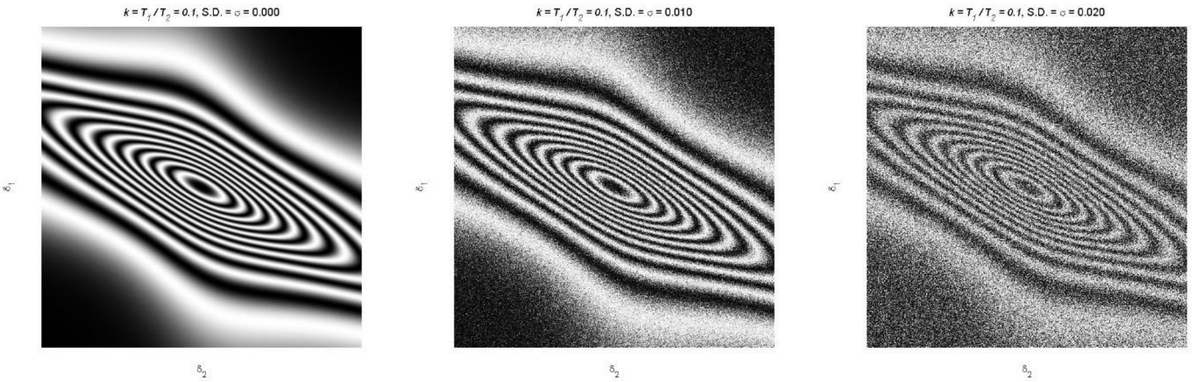

(a) (b) (c)

Figure 7(a) – (c). Qualitative contour plot of the RTOM signal intensity for $k = 0{,}1$ with noise given by a Standard Deviation, $\sigma = 0{,}000;\ 0{,}010$ and $0{,}020$

Table 3. Parameter estimate of $k = T_1/T_2$ for noisy data and fixed $\delta_1 = 0.50$

		k	**0.10**		**1.00**		**10.00**	
Data Set	**Standard Deviation**	**Number of Data Points**	**Number of Iterations**	**Parameter Estimate**	**Number of Iterations**	**Parameter Estimate**	**Number of Iterations**	**Parameter Estimate**
1	0,0000	41	25	0,1000	31	1,0000	32	10,0000
2	0,0009	41	35	0,1000	41	0,9993	38	9,9816
3	0,0050	41	36	0,1106	37	0,9950	42	9,9326
4	0,0100	41	36	0,1357	41	1,0001	43	9,8231
5	0,0200	41	43	0,0605	40	0,9887	41	9,5843
6	0,0300	41	45	0,0000	40	0,9962	44	8,3216
7	0,0350	41	46	0,0000	43	0,9419	47	11,1738
8	0,0500	41	40	0,1885	44	0,9459	45	10,9790

Once these values were calculated an estimate of the ratio of relaxation times k with values of *0,1*; *1,0* and *10,0* was obtained for each sub-region. To represent these values graphically, the absolute value of the difference between the actual k and the estimate of k is used to obtain a representative value of an estimate of the error in each sub-region. A gray level value is assigned to this estimate of the error, where a zero difference is white and increasing levels of gray represent a greater estimate of the error. Also shown, on the left side of each of these figures, is the corresponding contour diagram identifying the relationship between the contour map of normalized intensity and the sub-regions of interest. A general observation is that the best estimates of k, identified in white, roughly correspond to the main areas that occupy the normalized intensity contour maps. A finer sub-division of the area encompassing the contour map might yield the best regions from which data sets might be acquired when doing experimentation. Also, when comparing the contour maps shown of the left side of Figures 8 – 10 note that the longer axis of each contour map rotates counterclockwise as k increases. Additionally the shape changes from being wide and elongated to a more compact shape, and finally to being narrow and less elongated.

4. SUMMARY AND CONCLUSIONS

The purpose of this paper is to propose an inverse problem methodology that encompasses both a simulation side and an experimental side, to attempt to achieve the age old goal of combining experimentation with analytical/numerical approaches. The simulation side is used to not only solve a forward problem related to nonlinear op-tics to determine the dependence of the Rayleigh-type optical mixing (RTOM) normalized signal intensity on the incident pump and probe frequencies for different values of the ratio of relaxation times $k = T_1/T_2$. But to recover the ratio of the relaxation times k from consideration of sparse and/or noisy incident pump and probe frequency data sets in solving an inverse problem from which the full field RTOM signal intensity is reconstructed. The insights gained from this simulated forward and inverse problem solution, which may be effectively viewed as a form of analytical/numerical experimentation, influences how an experimental forward problem may be set up and con-ducted to maximize its effectiveness in terms of efficiency and time.

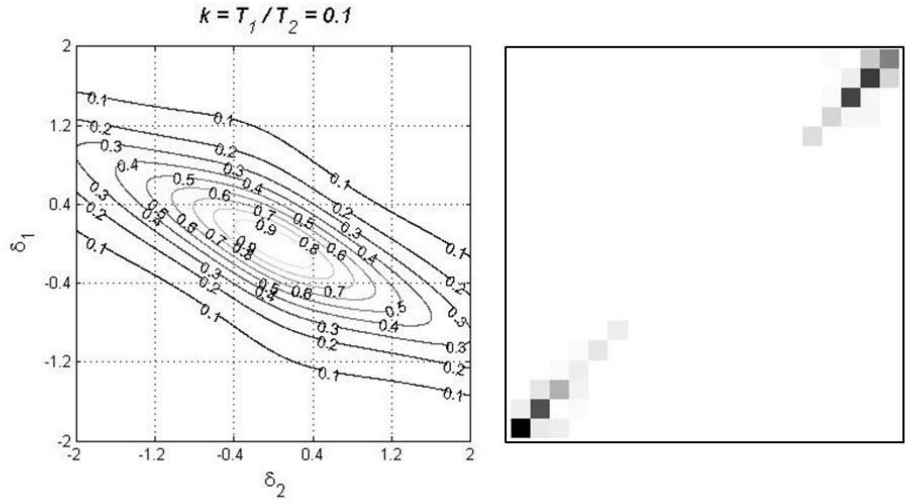

Figure 8. Contour plot of the RTOM signal intensity for $k = 0{,}1$ and the corresponding error estimation

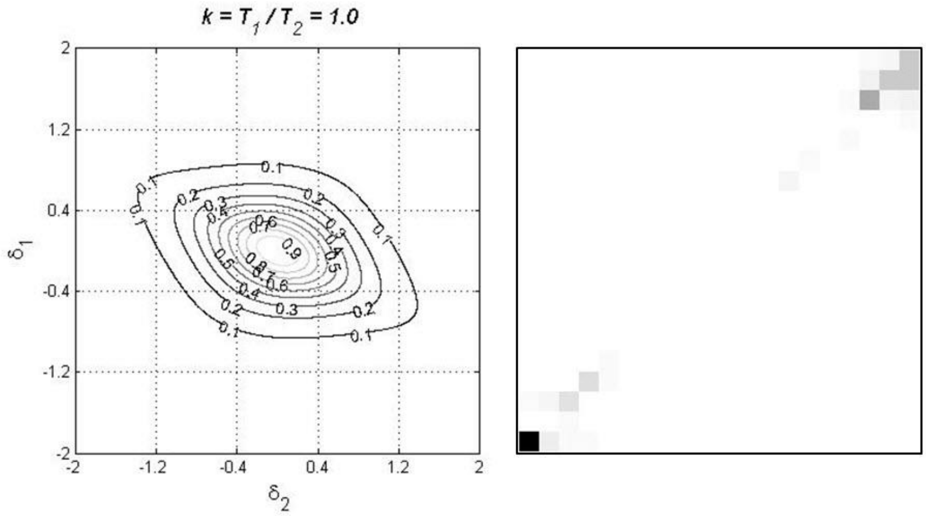

Figure 9. Contour plot of the RTOM signal intensity for $k = 1{,}0$ and the corresponding error estimation

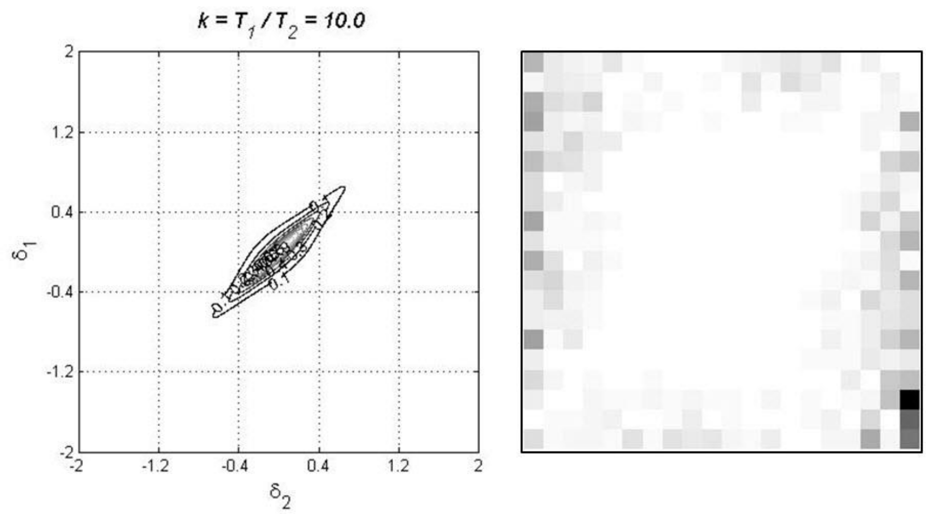

Figure 10. Contour plot of the RTOM signal intensity for $k = 10{,}0$ and the corresponding error estimation

In summary, an inverse problem methodology is defined to determine the ratio of the relaxation times k from values of normalized RTOM signal intensity where data sets of different sizes, noisy data sets and data sets from different sub-regions have been used to assess the robustness of the inverse problem methodology. The results point to a robust procedure which has the potential to influence efficient experimental application, which will be pursued in the near future.

ACKNOWLEDGEMENTS

JFC-G and JLP acknowledge the financial support provided by the SENESCYT-Ecuador through the Prometeo Project.

REFERENCES

Franco, H. J., Paz, J. L., Reif, I., Marcano O., A. & Salazar, M. C. (1990). Symmetry properties of the Rayleigh-type optical mixing signal in frequency space. *Journal of the Optical Society of America B*, 7 (1), 57-63. http:/dx.doi.org: 10.1364/JOSAB.7.000057

Garcia Golding, F. & Marcano O., A. (1985). High-order effects in Rayleigh-type optical mixing. *Physical Review A*, 32, 1526-1530. http://dx.doi.org/10.1103/PhysRevA.32.1526

Haroche, S. & Hartman, F. (1972). Theory of Saturated-Absorption Line Shapes. *Physical Review A*, 6, 1280-1299. http://dx.doi.org/10.1103/PhysRevA.6.1280

Hartley, H. O. (1961). The Modified Gauss-Newton Method for the Fitting of Non-Linear Regression Functions by Least Squares. *Technometrics*, 3(2), 269-280. http://dx.doi.org/10.1080/00401706.1961.10489945

Marquardt, D. W. (1963). An Algorithm for Least-Squares Estimation of Nonlinear Parameters. *Journal of the Society for Industrial and Applied Mathematics*. 11(2), 431-441. http://dx.doi.org/10.1137/0111030.

Masumoto, Y., Shionoya, S., & Okamoto, H. (1985). Ultrafast relaxation of excitons in GaAs-AlAs multi-quantum-well structures studied by resonant Rayleigh-type optical mixing. *Optical Communications*. 53, 385-388. http://dx.doi.org/10.1016/0030-4018(85)90023-9.

Paz, J. L., Franco, H. J., Reif, I., Marcano O., A. & Garcia Golding, F. (1988). Pump-power dependence due to parametric amplification of the Rayleigh-type optical-mixing signal. *Physical Review A*, 37 (9), 3381-3385. http://dx.doi.org/10.1103/PhysRevA.37.3381

Souma, H., Yajima, T. & Y. Taira (1980). Ultrafast Relaxation Study by Resonant Rayleigh-Type Mixing Spectroscopy Using Picosecond Light Pulses. *Journal of the Physical Society of Japan*, 48, 2040-2047. http://dx.doi.org/ 10.1143/JPSJ.48.2040.

Souma, H., Heilweil, E. J., & Hochstrasser, R. M. (1982). Resonant nonlinear optical mixing using the phase conjugate configuration: Spectroscopic studies. *The Journal of Chemical Physics*, 76, 5693-5702. http://dx.doi.org/10.1063/1.442990

Yajima, T. & Souma, H. (1978). Study of ultra-fast relaxation processes by resonant Rayleigh-type optical mixing. I. Theory. *Physical Review A*, 17, 309-323. http://dx.doi.org/10.1103/PhysRevA.17.309.

Yajima, T., Souma, H. & Ishida, Y. (1978). Study of ultra-fast relaxation processes by resonant Rayleigh-type optical mixing. II. Experiment on dye solutions. *Physical Review A*, 17, 324-334. http://dx.doi.org/10.1103/PhysRevA.17.324.